Sensors and Actuators B xxx (2011) xxx–xxx

Contents lists available at ScienceDirect

Sensors and Actuators B: Chemical

journal homepage: www.elsevier.com/locate/snb

Luminescent Eu(III) hybrid sensors for in situ copper detection

Beatriz C. Barja [a,*], Sara E. Bari [a], M. Claudia Marchi [a,b], Fabricio L. Iglesias [c], Milagros Bernardi [c]

[a] INQUIMAE and Departamento de Química Inorgánica, Analítica y Química Física, Facultad de Ciencias Exactas y Naturales, Universidad de Buenos Aires, Ciudad Universitaria, Pabellón 2, C1428EHA Buenos Aires, Argentina
[b] Centro de Microscopías Avanzadas (CMA), Facultad de Ciencias Exactas y Naturales (FCEyN), Universidad de Buenos Aires, Ciudad Universitaria, Pabellón 1, C1428EHA Buenos Aires, Argentina
[c] Departamento de Química Inorgánica, Analítica y Química Física, Facultad de Ciencias Exactas y Naturales, Universidad de Buenos Aires, Ciudad Universitaria, Pabellón 2, C1428EHA Buenos Aires, Argentina

ARTICLE INFO

Article history:
Received 9 February 2011
Received in revised form 19 May 2011
Accepted 1 June 2011
Available online xxx

Keywords:
Hybrid materials
Sol–gel
Europium(III)
Luminescence quenching
Cu(II) sensor

ABSTRACT

In this work we used the sol–gel technique to develop luminescent Eu(III) transparent films deposited on glass slides to build for sensor devices capable of monitoring transition metal ions in aqueous solutions. The films were obtained from a bis(trialkoxysilyl) organic precursor synthesized from the amide of the 2,6-pyridinedicarboxylic acid (DPA) with aminopropyltriethoxysilane (APTES) in the presence or absence of cetyl trimethyl ammonium bromide (CTAB) surfactant as templating agent and triethylethoxysilane (TEOS) as crosslinker. These sensor devices were used to perform in situ quenching experiments by Cu(II), Fe(III), Co(II) and Ni(II) ions. The results indicate that the templated films allow the detection and quantification of these metals down to ppb levels by means of the values of the Stern–Volmer constants. In particular, it was shown that Cu(II) acts as an extremely efficient quencher ($K_{SV} = 3.5 \times 10^5\ M^{-1}$) when compared with the results obtained for the other metals, opening the possibility to use these devices as potential Cu(II) sensors for actual applications in aqueous media.

1. Introduction

The use of bridged silsesquioxanes $[(RO)_3Si]_n - R'$ $(n \geq 2)$ as precursors to include an organic functional group inside the inorganic framework of a mesoporous matrix itself gave rise, since the pioneering works in the early nineties, to the novel periodic mesoporous organosilicas (PMO) [1–3]. The development of luminescent PMO is in constant progress [4]. The functionalization of these matrices with different organic groups capable of emitting light efficiently is a key strategy. The increasing use of chemically modified bridged silsesquioxanes, to include lanthanides by the sol–gel technique into the frameworks and/or the pores of the hybrid matrices [5–7] in order to obtain lanthanide based luminescent organic–inorganic hybrid materials can be attributed to the high potential of these materials for several applications as sensors, organic light emitting diodes, phosphors, etc. [8,9].

Lanthanide ions display a well-defined luminescence characterized by narrow and highly structured emission bands arising from their parity forbidden intra f–f transitions. Their excited state lifetimes are in the millisecond timescale and are not quenched by molecular O_2 [10–13], in contrast to what is generally observed for organic dyes. Unfortunately, their low absorption coefficients ($\varepsilon < 10\ M^{-1}\ cm^{-1}$) do not allow their use as such, but are useful when coordinated to an antenna chromophore capable of sensitizing the lanthanide emission mechanisms by populating the ion centered emitting states [14–16] through energy transfer. These unique properties focused the attention of many researchers in the design of different lanthanides complexes for potential applications as biological probes [17,18] or chemical sensors [19–21]. A recent review describes the latest developments in the use of lanthanides in a wide group of functional luminescent materials [22].

Europium based luminescent organosilica materials obtained by the hydrolysis and condensation of organoalkylsilanes from a sol–gel technique [23,24] have been widely used to immobilize organic or inorganic molecules [25–27] in a porous glass or film [28] or nanoparticles [29] to build optical sensors of pH [30], anions [21] and cations [31,32].

Transition metal ions are known to be efficient quenchers of the emission of lanthanide complexes being the electronic energy transfer the deactivating mechanism postulated to operate in these cases [33,34].

Among these metals, Cu (II) ions act much more efficiently than any other fourth period transition metal cation [35,36]. The sodium salt of the tris 2,6-pyridinedicarboxylic Eu(III) complex, $Na_3Eu(DPA)_3$, has the advantage that the DPA acts not only as an efficient coordinating ligand, but also as an antenna enhancing the emission intensity and therefore the sensitivity of the luminescent system towards the detection of cations. A recent

* Corresponding author. Fax: +54 11 4576 3341.
E-mail address: barja@qi.fcen.uba.ar (B.C. Barja).

0925-4005/$ – see front matter © 2011 Elsevier B.V. All rights reserved.
doi:10.1016/j.snb.2011.06.006

publication reports the luminescence quenching of $Na_3Eu(DPA)_3$ and $Na_3Tb(DPA)_3$ in aqueous solution for the detection of Fe(III) [37]. Other authors synthesized a metal-organic framework (MOF) using a luminescent Eu(III)–3,5-pyridinedicarboxylic acid–dimethylformamide complex for which Cu(II) showed the most significant quenching effect [38].

The technology applied to the development of metal sensors is in constant progress with the purpose of attaining lower detection limits and higher specificity for the different analytes. Luminescence based analytical methods are known to be one of the most sensitive techniques and this advantage has been widely used to develop optical sensors for the detection of different analytes, including Cu(II) [39–41].

The use of expensive and generally sophisticated instrumentation makes the detection not suitable for an in situ or on-line monitoring, particularly if the sample needs special treatments such as preconcentration. In this work, we use the sol–gel technique to synthesize luminescent transparent Eu(III) films from a bis(trialkoxysilyl) organic precursor synthesized from the diamide of 2,6-pyridinedicarboxylic acid (DPA) with aminopropyltriethoxysilane (APTES) in the presence or absence of cetyltrimethyl ammonium bromide (CTAB) surfactant with triethylethoxysilane (TEOS) as crosslinker. The films were deposited on glass slices to build solid devices that operate by measuring the decrease in the emission signal of the $Eu(III)(DPA)_3$ complex in the presence of a transition metal. At this point it is worth mentioning that, contrary to what is usually reported, these devices were constantly immersed in the solution to be tested while simultaneously measuring the signal response. Therefore, the films deposited in the glass slides of these devices have the adequate mechanical robustness and chemical stability for in situ detection during long periods of time. The performance of these devices as potential sensors of Cu(II) was evaluated in terms of the values of the Stern–Volmer constant of the quenching experiments. This equation has been widely used to evaluate the relationship between the relative fluorescence intensity of an immobilized luminescent probe and the measured analyte concentration; coated fiber sensors, enzyme-mediated sensors, or gas sensors are representative examples [42]. These low cost simple devices are capable of sensing Cu(II) down to 50 ppb in aqueous systems for which neither pretreatment, degasification nor destruction of the sample are necessary.

2. Materials and methods

2.1. Chemicals

Copper(II) chloride-dihydrate, cobalt(II) nitrate hexahydrate, nickel(II) chloride hydrate, iron(III) nitrate nonahydrate, DPA (2,6-pyridinedicarboxylic) acid, APTES (3-aminopropyltriethoxysilane), TEOS, and CTAB (cetyltrimethylammonium bromide) were obtained from Aldrich. All compounds were analytical grade and were used without further purification. $Eu(NO_3)_3{\cdot}6H_20$ (99%) was obtained from Fluka Chemie AG and used as received. Water was from a Milli-Q system. $Na_3Eu(DPA)_3{\cdot}15H_2O$ was synthesized according to literature methods [43]. HCl(c) and NH_3(c) were from Mallinckrodt.

2.2. Spectroscopic measurements

Steady State emission spectroscopy: The steady state emission spectra were recorded on a PTI QuantaMaster QM-1 luminescence spectrometer. The excitation and emission wavelengths were 290 nm and 615 nm, respectively. Excitation and emission bandwidths were set to 8 and 4 nm, respectively. The experimental points plotted in the graphs of the quenching experiments were obtained from the emission intensity averaged over a period of 10 min. These average values were affected by an error not higher than 3%.

Infrared spectroscopy: IR spectra were obtained in KBr pellets using a Nicolet 8700 FTIR equipment.

2.3. Microscopic measurements

Scanning electron microscopy (SEM) was performed on a Zeiss Supra 40 microscope equipped with a field emission gun (CMA, FCEN-UBA). The images were taken with in-lens detector and 3 kV acceleration voltages. The samples were placed on an aluminum holder, supported on conductive carbon tape.

2.4. Synthesis of the compounds

A prehydrolized stock solution of TEOS, ethanol, water and HCl ($1{:}3.63{:}1{:}4.75 \times 10^{-5}$ molar ratio) was refluxed for 90 min at 60 °C. An organic hybrid N,N-bis(triethoxysilanepropyl)-2,6-pyridine dicarboxiamide ligand (SL, M = 573 g mol^{-1}) synthesized according to published procedures [44,45] was added to the stock solution (nSL:nTEOS = 1:15.5) in HCl 7 mM under stirring. After 45 min of ageing, the sol was diluted in ethanol (nSi:nEtOH = 1:26.5) to achieve the final molar ratio nSi:nEtOH:nwater:nHCl = $1{:}26.5{:}5.23{:}3.95 \times 10^{-3}$ [46]. CTAB was added under stirring to half of the sol as a structuring agent in a 4.1% (w/w). $Eu(NO_3)_3$ was added to both sols with a molar ratio of nSL:nEu(III) = 1:2.9 (in the absence of CTAB added) and nSL:nEu(III) = 1:3.0 (for templated films with CTAB). The synthetic procedure is depicted in Scheme 1.

2.5. Fabrication of the sensors

The sensors were fabricated by dip-coating clean glass slides (0.8 cm × 3.8 cm × 1 mm) into the sols synthesized as described in Section 2.4, at a constant pulling rate of 10 cm/min to obtain transparent films which were left ageing at room temperature for 3 months in sealed boxes. A further heating at 95 °C for 24 h was performed for a better structuration. A sketch of the hybrid material is depicted in Scheme 2.

The CTAB was removed from the templated films by heating them with ethanol at 65 °C for 2.45 h. FTIR spectra of the films were registered to track the presence of CTAB until the ν_{CH2} bands located at 2800–3000 cm^{-1} were significantly reduced. Residual signals in this region are assigned to the methylene groups of the synthetic material. After the CTAB was withdrawn, the sensors were placed in an oven at 60 °C overnight. Hereafter, the films with and without CTAB will be named templated sensors (TS) and non-templated sensors (NTS) films, respectively.

2.6. Luminescence measurements with the sensors

The sensors were firmly fixed to a specially designed cuvette half cap. This cap keeps the sensor in a front face geometry (55° approximately) inside the cuvette which is filled with the solution of the test sample. The luminescent response was measured in situ, with the sensors always immersed in the solution and kept in the spectrofluorimeter in the same position. The sensor was allowed to equilibrate with water (hydration period) before recording the zero quencher intensity (I_o, no metal added). The addition of the metal quencher solution was performed from the top of the cuvette using a Hamilton microsyringe under stirring while keeping the cuvette with the sensor in the spectrofluorometer.

The steady state emission intensity of each sample was recorded at 615 nm after 500 s under stirring.

Please cite this article in press as: B.C. Barja, et al., Luminescent Eu(III) hybrid sensors for in situ copper detection. Sens. Actuators B: Chem. (2011), doi:10.1016/j.snb.2011.06.006

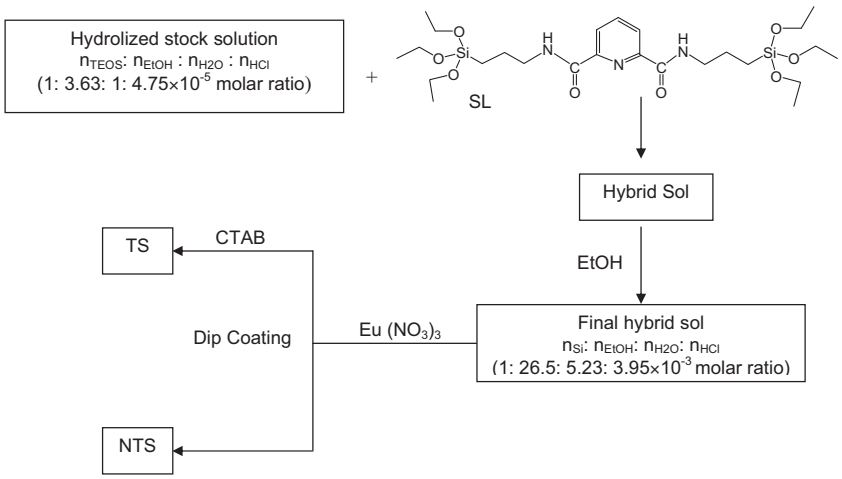

Scheme 1. Synthetic procedure.

3. Results and discussion

3.1. Infrared spectroscopy

Fig. 1 shows the infrared spectra of a film of a NTS and a TS sensor before and after the extraction of the template with ethanol. After the extraction, the spectra show a significant decrease in the bands located at 2800–3000 cm^{-1} assigned to the C–H stretching modes of the CTAB. The remaining absorbance corresponds to the aliphatic streching modes of the synthetic material. The broad absorption band located in the range 1000–1200 cm^{-1} is assigned to the stretching of the Si–O–Si arising from the hydrolysis and condensation reactions of the silanized ligand and TEOS and these modes overlap with the bands associated with Si–O–C, Si–C stretchings. The bands located at ca. 440 cm^{-1} and 800 cm^{-1} are assigned to the $\rho_{Si-O-Si}$ and $\nu_{sym\ Si-O-Si}$ modes, respectively while those at 950 cm^{-1} correspond to the ν_{Si-OH} mode.

The ν_{CO} (amide I) values for the hybrid moiety of the TS and NTS sensors appear at 1631 cm^{-1} and 1641 cm^{-1}, respectively. These values are in the wavelength range reported for aromatic amide complexes of Eu(III) (ν_{CO} = 1610–1651 cm^{-1}) [47,48].

The amide II band, a mixed vibration of the NH in plane deformation coupled to the C–N stretching ($\delta_{NH} - \nu_{CN}$), absorbs at 1560 cm^{-1} in both films, in agreement with the values expected for the trans configuration for a secondary amide (1550 ± 50 cm^{-1}) [49].

3.2. Emission properties of the NTS and TS films

The emission spectra of the dry TS and NTS sensors show the characteristic Eu(III) centered transition bands ($^5D_0 \rightarrow {}^7F_J$) for J = 0, 1, 2, 3, and 4 at ca. 578, 590, 615, 650, and 698 nm, respectively (Fig. 2). The intensity of the spectra when excited at 290 nm (absorption maximum of the DPA ligand) is more than one order of magnitude higher than the intensity of the spectra

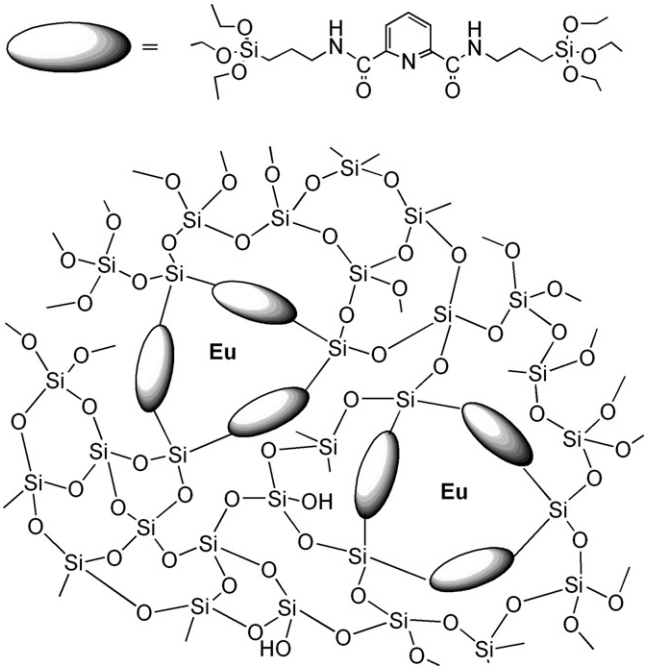

Scheme 2. Sketch of the hybrid material. SL is the silanised ligand (N,N-bis(triethoxysilanepropyl)-2,6-pyridine dicarboxiamide ligand).

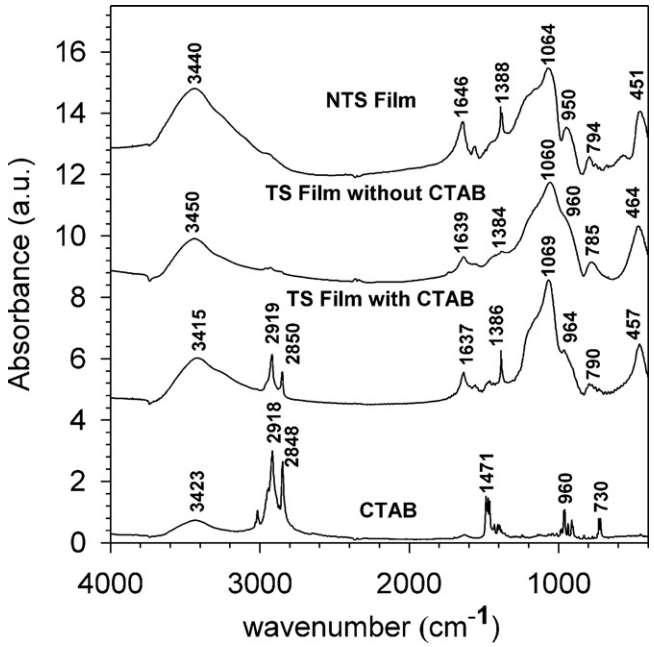

Fig. 1. Infrared spectra of a film of a NTS and a TS sensor before and after the extraction of the template with ethanol.

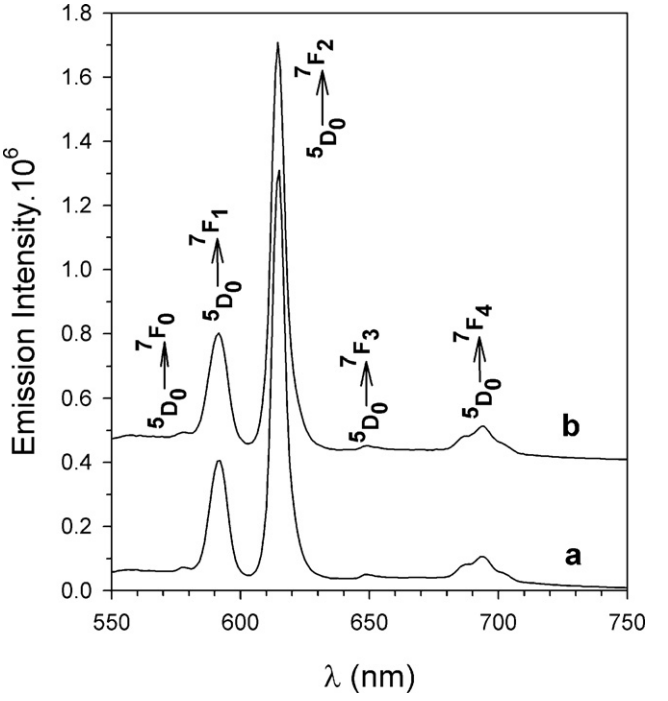

Fig. 2. The emission spectra of the dry TS and NTS sensors show the characteristic Eu(III) centered transition bands ($^5D_0 \rightarrow {}^7F_J$) for J = 0, 1, 2, 3, and 4 at ca. 578, 590, 615, 650, and 698 nm, respectively.

when excited at 394 nm (absorption band of the Eu(III) ion, not shown), indicating that the DPA moiety efficiently coordinates the sites of the first coordination sphere of the Eu(III), and that the antenna effect from the DPA to the Eu(III) is conserved in the films.

The ratio of the intensities for the ($^5D_0 \rightarrow {}^7F_2$) to that of the ($^5D_0 \rightarrow {}^7F_1$) is I_{F2}/I_{F1} = 3.8 for both types of sensors. This value is in good agreement with the one obtained in the emission spectrum of the solid $Na_3Eu(DPA)_3$ complex (I_{F2}/I_{F1} = 3.2). The higher this ratio, the lower is the symmetry of the local environment of the Eu(III) ions in the matrix [50]. These results indicate that the Eu(III) ions sense similar environments when they are located in the hybrid silica-DPA films or in the solid $Na_3Eu(DPA)_3$ complex. In both cases, the site symmetry of the Eu(III) center lowers from the pure solid complex to an C_s or even lower point-group symmetry in glasses [50].

3.3. Microscopy measurements

Fig. 3 shows the SEM micrographs of the transparent TS and NTS films and of the powders obtained by scratching their surfaces.

In the images obtained for the NTS films at small magnification (Fig. 3a), square shaped particles were observed immersed in an uniform framework with no visible interstitial voids (inset of Fig. 3a). These particles (20–200 nm) can be associated with the phenyl-bridged polysilsesquioxanes as they suffer from degradation under exposure to the electron beam. When the films were scratched, the SEM images revealed their morphology. The cross section of the film showed an internal structure composed of pores and particles in the range of 5 nm average (Fig. 3c).

When the templated films were analyzed at small magnification (Fig. 3b), irregularly shaped particles were observed immersed in a matrix with a higher degree of porosity than the NTS films (inset of Fig. 3b). It is observed from the SEM images of the TS films that the

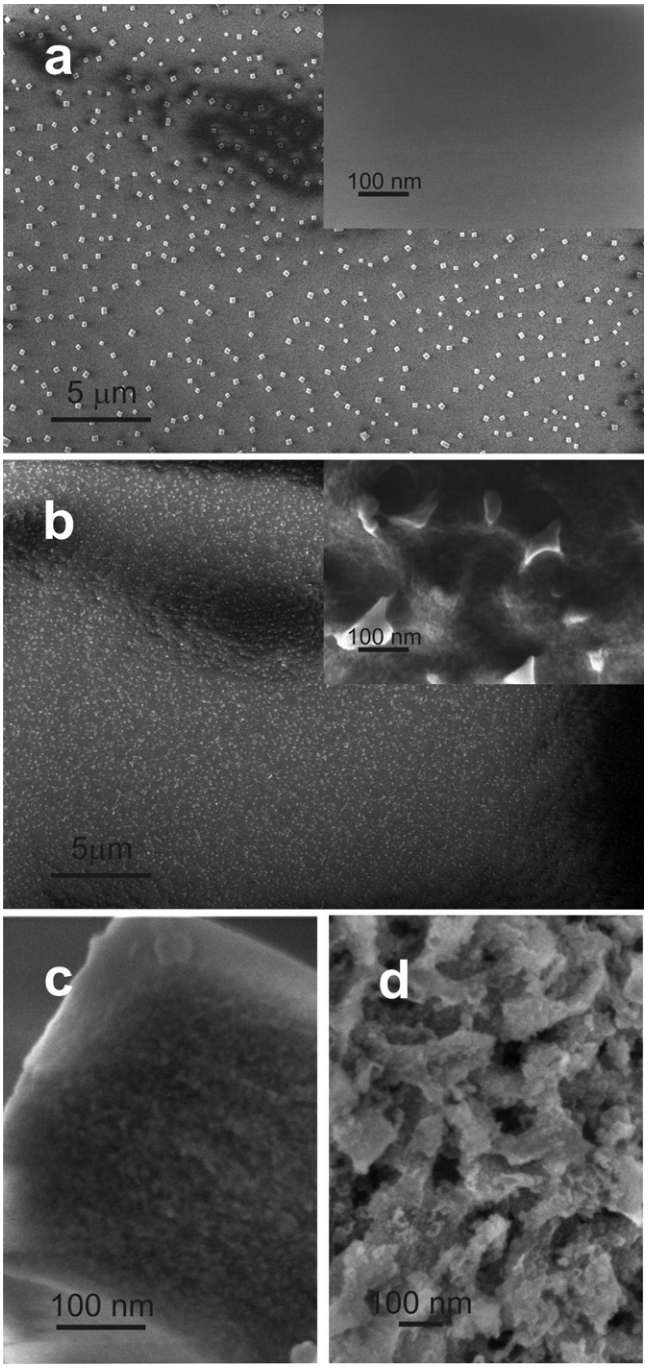

Fig. 3. Scanning electron microscopies (SEM) of (a) NTS films and (b) TS films supported on glass for low magnification (scale bar = 5 μm). Their insets show the detail at higher magnification (scale bar = 100 nm). SEM of the powders obtained by scratching the surfaces of: (c) the NTS films, (d) TS films at high magnification (scale bar = 100 nm).

inclusion and later extraction of the template (CTAB) did influence the structure of the films. The hybrid particles changed their shapes and distribution as a result of this inclusion. In Fig. 3d, the cross section of the templated film shows a more open structure than in Fig. 3c for the NTS films.

The differences in these morphologies can be attributed to changes in the spatial geometry of the large bis(trialkoxysilyl amide of the dipicolinic acid precursor in the hybrid silica network. These results affect the adsorption properties as revealed from the accessibility of the metals in the quenching experiments.

Please cite this article in press as: B.C. Barja, et al., Luminescent Eu(III) hybrid sensors for in situ copper detection. Sens. Actuators B: Chem. (2011), doi:10.1016/j.snb.2011.06.006

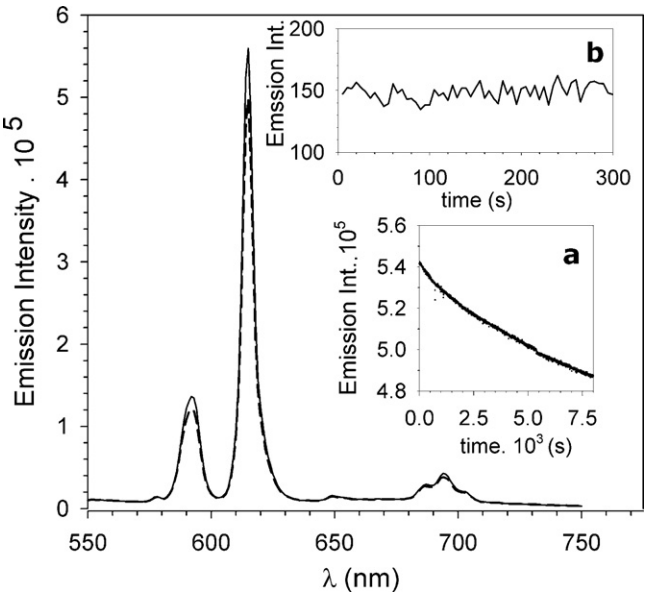

Fig. 4. Luminescence spectra of a dry NTS (solid line) and a hydrated one (dashed line). Inset (a): decrease of the signal at the maximum of the spectra (615 nm) during the hydration period with time. Inset (b): emission intensity at the maximum of the spectra (615 nm) as a function of time for the hydration water. For all measurements, λ_{exc} = 290 nm was used.

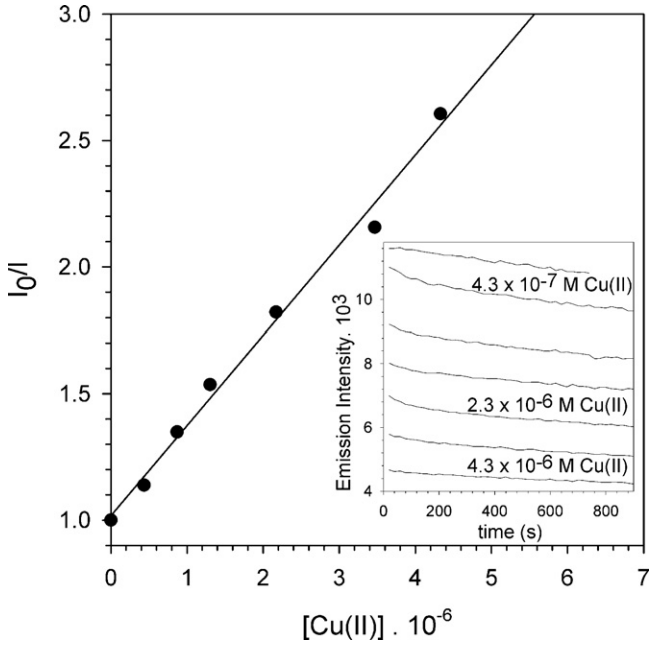

Fig. 5. Stern–Volmer plot for the deactivation of a TS film by Cu(II), [Cu(II)] = mol L^{-1}. Inset: decrease in the luminescent signal at the maximum of the emission spectra (615 nm) by the addition of Cu(II) with time. The Stern–Volmer plot constant is 3.5×10^5 mol^{-1} L.

3.4. Quenching experiments

3.4.1. Hydration

Dry NTS and TS films were immersed in water and left to equilibrate before any addition of metal quencher. Similarly to what happens to the glass electrode in pH meters, the films hydrate when put in contact with water causing the decrease in the intensity of the emission with time, while keeping the same spectrum profile (Fig. 4). The decrease in the intensity at the maximum of the emission spectrum of the films (615 nm) in water measured as a function of time is shown in Fig. 4, Inset a. All NTS and TS films show this typical hydration response which takes several hours before constant emission intensity is achieved (I_o).

To assess that the decrease in the intensity of the signal in water was due to the hydration process of the matrix and not to the leaching of the luminescent Eu(III) center to the solution, the emission response of the hydration water at 615 nm was also measured with no sensor in place (Fig. 4, Inset b) and no trace of Eu(III) was observed. This indicates that no leaching of the Eu(III) to the aqueous solution occurs, as expected for a ligand covalently bounded to the silica matrix, and that the hydration process is responsible for the decrease of the signal. In addition it was observed that the hydration process was in average three times faster for TS than for NTS films indicating a better access of the water molecules to the luminescent Eu(III) center.

3.4.2. Luminescence quenching experiments

Once the NTS or TS films were hydrated and the I_o (no metal) value was measured, microliters of a concentrated quencher metal solution were added to the cuvette under stirring. After each addition of metal, the sensor was left to equilibrate again until an average value of the intensity was obtained within a 2% experimental error. No trace of free Eu(III) was observed in solution after the addition of the metal. The experiments were performed for the transition elements of the triad IIIB:Fe(III), Co(II) and Ni(II), and for Cu(II). Alkaline, earth alkaline and Cd(II) ions were tested in aqueous solution but no quenching of the luminescent signal was observed for concentrations higher than mmol L^{-1}, indicating that these cations do not interfere with the metals studied in this work.

3.4.3. Quenching measurements with TS films

The Stern–Volmer plot for the deactivation of the emission of the Eu(III) in the TS films by Cu(II) is shown in Fig. 5, and those for Fe(III), Co(II) an Ni(II) are shown in Fig. 6. Linear Stern–Volmer plots were obtained for the four ions for similar I_o/I ratios.

The Stern–Volmer constants (K_{sv}) obtained are 3.5×10^5 M^{-1}, 8.0×10^3 M^{-1}, 6.3×10^3 M^{-1} and 4.1×10^3 M^{-1} for Cu(II), Ni(II),

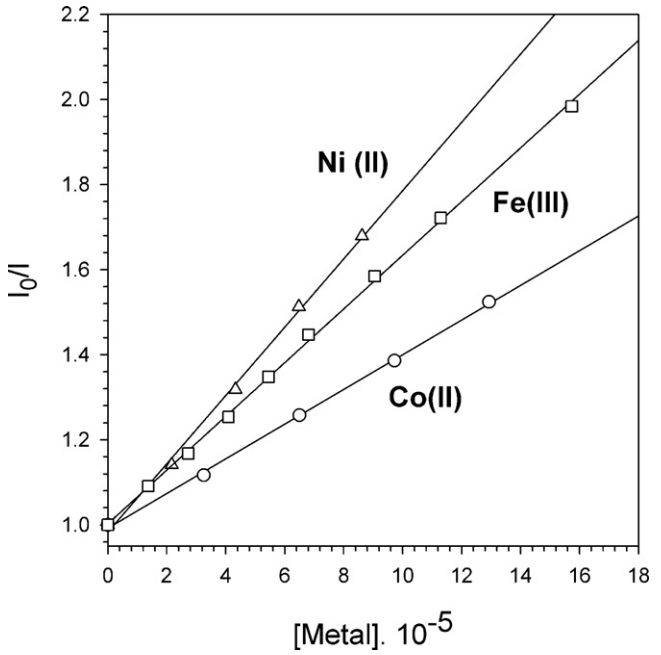

Fig. 6. Stern–Volmer plots for the deactivation of TS films by Ni(II), Fe(III) and Co(II) in aqueous solution ([Me] = mol L^{-1}). The corresponding Stern–Volmer constants are: 8027, 6313, and 4075 mol^{-1} L in the same order.

Please cite this article in press as: B.C. Barja, et al., Luminescent Eu(III) hybrid sensors for in situ copper detection. Sens. Actuators B: Chem. (2011), doi:10.1016/j.snb.2011.06.006

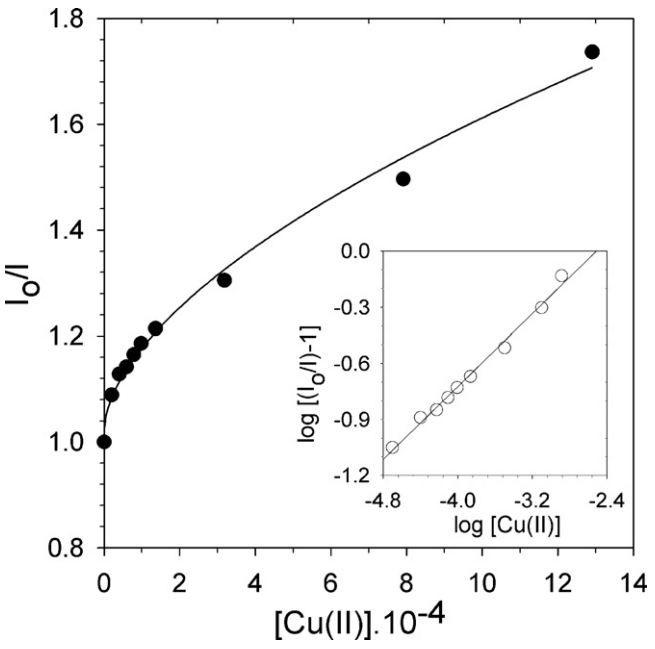

Fig. 7. Stern–Volmer plot for the quenching of a NTS film by Cu(II), [Cu(II)] = mol L^{-1}. Inset: logarithmic plot of a Freundlich isotherm according to the equation: $\log[(I_o/I) - 1] = 0.49 \log[\text{Cu(II)}] + 1.23$.

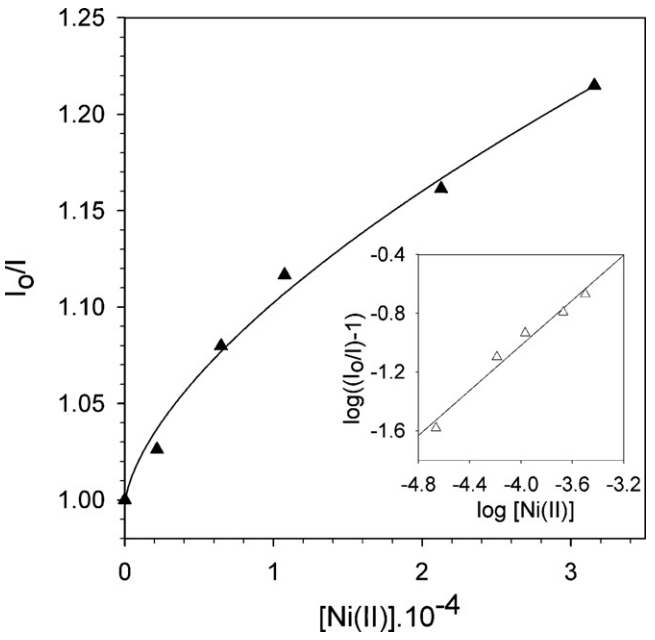

Fig. 8. Stern–Volmer plot for the quenching of a NTS film by Ni(II), [Ni(II)] = mol L^{-1}. Inset: logarithmic plot of a Freundlich isotherm according to the equation $\log[(I_o/I) - 1] = 0.77 \log[\text{Ni(II)}] + 2.06$.

Fe(III) and Co(II), respectively. It is clear from these results that Cu(II) is by far the most efficient quencher, as the Stern–Volmer constant is two orders of magnitude higher than the rest of the metals.

The recovery of the initial value I_o, by thoroughly rinsing with water, was possible for all the metals except for Cu(II), in which case only a 40–50% recovery was attained.

3.4.4. Quenching measurements with non templated sensors (NTS)

Luminescence quenching experiments by Cu(II), Fe(III), Co(II), and Ni(II) were performed in aqueous solution at room temperature with the NTS films. Contrary to what is observed with the TS films, the Stern–Volmer plots for Cu(II), Ni(II) and Fe(III) (Figs. 7–9, respectively) show a non linear dependence of I_o/I with the concentration of the metal quencher. In the case of Co(II) (Fig. 10), the Stern–Volmer plots are almost linear and the downward curvature is not always observed.

We found that the experimental data can be fitted to a Freundlich adsorption isotherm:

$$[\text{Me}]_{\text{film}} = K_f[\text{Me}]^{1/n} \quad (1)$$

$[\text{Me}]_{\text{film}}$ is the metal concentration adsorbed in the film, K_f is the Freundlich adsorption constant which indicates the sorption affinity and $1/n$ is an experimental dimensionless heterogeneity parameter which controls the non-linearity of the isotherm. The Freundlich sorption model considers scenarios where the number of sorption sites relative to the number of solute molecules is very large (assumed unlimited). This is the case for very dilute solutions and therefore the model can be applied for the metal concentrations studied in this work.

Taking into account this dependence, the Stern–Volmer given by Eq. (2)

$$\frac{I_o}{I} = K_{sv}[\text{Me}] + 1 \quad (2)$$

can be rewritten as:

$$\frac{I_o}{I} - 1 = K_{sv}K_f[\text{Me}]^{1/n} \quad (3)$$

$$\log\left(\frac{I_o}{I} - 1\right) = \frac{1}{n} \log[\text{Me}] + \frac{1}{n} \log K_{sv}K_f \quad (4)$$

The data were plotted in the logarithmic form, Eq. (4), and are shown in the insets of Figs. 7–10.

Given the n values, the value for $K_{sv}K_f$ can be calculated from the ordinate of Eq. (4) for each metal (Table 1). If we take the K_{sv} values for the TS films, for which we assume that an adsorption process is

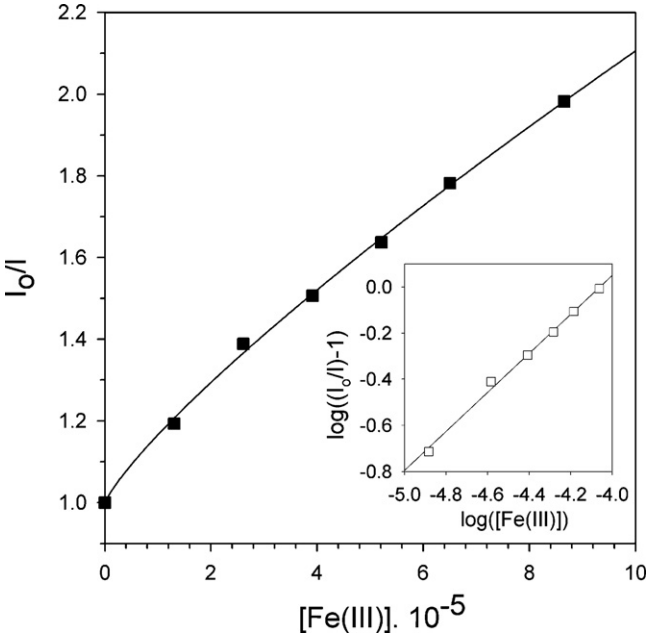

Fig. 9. Stern–Volmer plot for the quenching of a NTS film by Fe(III), [Fe(III)] = mol L^{-1}. Inset: logarithmic plot of a Freundlich isotherm according to the equation $\log[(I_o/I) - 1] = 0.84 \log[\text{Ni(II)}] + 3.4$.

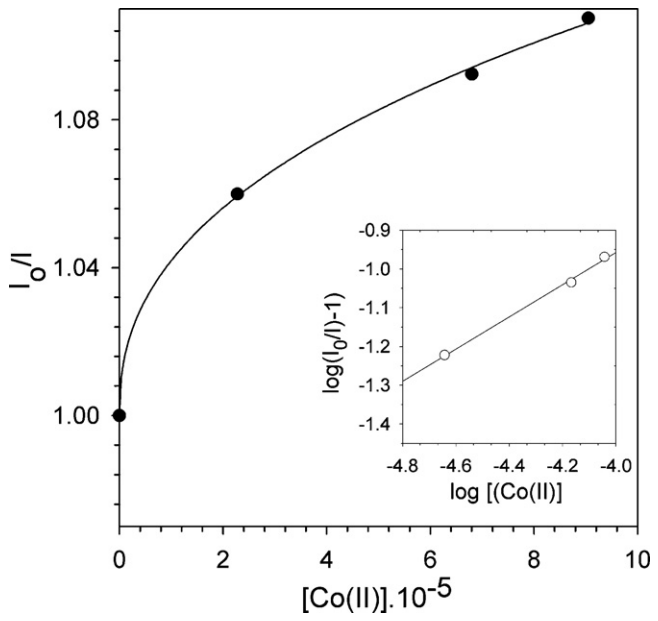

Fig. 10. Stern–Volmer plot for the quenching of a NTS film by Co(II), [Co(II)] = mol L^{-1}. Inset: logarithmic plot of a Freundlich isotherm according to the equation $\log[(I_o/I) - 1] = 0.42 \log[\text{Co(II)}] + 0.71$.

negligible, it is possible to predict roughly that the affinity of Fe(III) for the film surface is higher than for the rest of the metals. A larger K_f is expected given the favorable electrostatic interaction among the positive triply charged Fe(III) ions and the negatively charged silica in water.

Another point worth to be mentioned is that the NTS films recovered almost 100% of their original I_o value when they were washed out with water, independently of the metal. This fact supports the results in the sense that a physisorption process can be the mechanism responsible for the deactivation of the films by the metal quencher.

Therefore, non templated materials do not render the suitable porosity to allow a good accessibility of the ions inside the matrix of the NTS films, prevailing mostly the surface interaction between the luminescent centers of Eu(III) and the quencher metals. The description of the quenching process by a Freundlich isotherm also points out the heterogeneity of the surface of the hybrid NTS films.

3.4.5. Luminescence deactivation of Eu(III) complexes with metal ions

3.4.5.1. Aqueous solution. It has been known for a long time that heavy metals are efficient quenchers of luminescence. This quenching process may proceed from different mechanisms depending on the type of fluorophore. For the long ms lifetimes of luminescence of lanthanide ions, this is especially true. In a previous work [51], we measured the deactivation of several Eu(III) complexes by Cu(II), Ni(II) and Co(II) in aqueous solution. Static quenching was the main mechanism for ligands such as DPA in which very stable non luminescent 1:1 and 1:2 complexes were formed in solution with the metal quencher [52]. It is known from literature data that Cu(II) forms 1:1 and 1:2 complexes with DPA^{2-} as ligand, with $K_1 = 1.4 \times 10^9\ M^{-1}$ and $K_2 = 2.4 \times 10^7\ M^{-1}$. In the case of Co(II), the equilibrium constants for the 1:1 and 1:2 complexes with DPA are $K_1 = 4.2 \times 10^6\ M^{-1}$ and $K_2 = 1.1 \times 10^6\ M^{-1}$ [33]. The equilibrium constants for the 1:1 and 1:2 complexes of Ni(II) with DPA ligand are $K_1 = 8.9 \times 10^6\ M^{-1}$ and $K_2 = 3.5 \times 10^6\ M^{-1}$ [33]. For Fe(III) these values are $K_1 = 8.1 \times 10^{10}\ M^{-1}$ and $K_2 = 1.6 \times 10^6\ M^{-1}$ [53]. Taking into account the corresponding 1:1, 1:2 and 1:3 formation constants for the Eu(III) complexes with DPA^{2-} ($K_1 = 7 \times 10^8\ M^{-1}$, $K_2 = 1.4 \times 10^7\ M^{-1}$ and $K_3 = 3.2 \times 10^5\ M^{-1}$) [54], a cation exchange process is highly probable between Eu(III) and these transition metals leading to the deactivation of the luminescence.

Cu(II) showed an unusual deactivation efficiency when compared with the rest of the metals. This result is in good agreement with those reported by Kessler [35] for the luminescent deactivation of an Eu(III) terpyridine-derived complex by ten different metals in aqueous solution, including Ni(II), Co(II) and Fe(III). The postulated mechanism that operates in those cases is the electronic energy transfer from the metal quencher to the emissive lanthanide center [33,34].

3.4.5.2. Hybrid films. In the hybrid films the Eu(III) ions are entrapped in the matrix by coordination to the silanised ligands of the matrix. In a previous paper [45], we showed that for bulk Eu(III)-based silanised hybrid materials, the deactivation of the emission of the Eu(III) ions by Cu(II) was directly related with the number of water molecules located in the first coordination sphere of the lanthanide. If this number of sites is different from zero, they can be reached out by the metal quencher ions and replace the water molecules provoking the deactivation of the Eu(III) luminescence. In view of these facts, it is highly probable that the metal ions locate in these labile water-sites in the vicinity of the Eu(III) centers of the films deactivating the emission of the lanthanide. This would explain the observed reversibility of the sensors. In NTS and TS sensors the measurement of the water molecules was not possible, given that the luminescence was too weak to measure the decay lifetimes of the Eu(III) ions and therefore no calculation of the number of water molecules directly bounded to the Eu(III) center was performed.

Table 1
Stern–Volmer constants (K_{SV}) for the TS films. The parameters (K_{SV} K_f) and n were obtained from the ordinate and the slope of Eq. (4), respectively. K_f is the Freundlich adsorption constant and n is the inverse of the heterogeneity parameter.

	Fe(III)	Cu(II)	Ni(II)	Co(II)
n	1.3	2.0	1.3	2.5
K_{sv} [M^{-1}]	6.3×10^3	3.5×10^5	8.0×10^3	4.1×10^3
K_{sv} K_f [L/M g $mol^{(1-1/n)}$]	1.7×10^4	1.6×10^2	4.2×10^2	56

4. Conclusions

The results show that the deactivation of the emission of the films by Cu(II), Ni(II), Co(II) and Fe(III) strongly depends on the nature of the films. The inclusion of the CTAB as a structuring agent during the synthesis of the hybrid matrix of the sensors greatly enhances the sensibility (Stern–Volmer slopes) of the TS films when compared with the NTS ones.

For non templated films, only a fraction of the total Eu(III) ions (those that are in the surface of the material) can be reached out by the metal ions and hence deactivate the emission of the lanthanide. This quenching effect can then be fit in terms of a combination of a Freundlich isotherm with a static deactivation process dictated by the Stern–Volmer equation.

For the templated films, the metal ions can enter more easily inside the material due to the higher porosity of the matrix (shown in the micrographs in Fig. 3) facilitating the interaction of the incoming metal ions with the Eu(III) ions that are not only in the surface but also inside the matrix. The adsorption mechanism is not the limiting process now and the static deactivation of the luminescence is the main responsible of the quenching process.

We have previously observed that EuDPA-TEOS hybrid materials possess a much higher accessibility of Cu(II) ions into F127-templated matrices than for those with no template agent [45].

Please cite this article in press as: B.C. Barja, et al., Luminescent Eu(III) hybrid sensors for in situ copper detection. Sens. Actuators B: Chem. (2011), doi:10.1016/j.snb.2011.06.006

Materials with higher porosity facilitate the entrance of ions permitting a closer interaction with the target centers.

This is clearly reflected in the detection levels of the metals. TS films are capable of sensing down to 50 ppb of Cu(II) for a 10% of emission deactivation which is lower than the Maximum Contaminant Level (MCL) health standard set by the United States Environmental Protection Agency for drinking water (1.3 ppm). In the case of Ni(II), Co(II) and Fe(III) the detection values for a 10% of emission deactivation for TS films are 0.8 ppm, 1.4 ppm and 0.7 ppm, respectively in the same order of magnitude than the values regulated for drinking water. These films show a linear signal response with the addition of the metal quencher which provides a direct measurement of the metal cation making them easier to work with. In the case of the NTS, it is derived from the Stern–Volmer plots (Figs. 7–10) that the concentration of metal cation necessary for a 10% of deactivation ($I_0/I = 1.1$) falls in the range of 10^{-4} M (or 6 ppm for an average atomic number equal to 60 g mol^{-1} for the metal ion) and are not suitable for sub-ppm metal detection.

The fact that Cu(II) acts as an extremely effective quencher of Eu(III) encourages us to improve its detection system by using optical fibers coated with the luminescent Eu(III)-DPA hybrid material to easily collect the excitation wavelength and simultaneously send the analytical response to the detector. The size of the system represents an advantage in cases where the samples are not accessible to the operator. The work is under progress.

These results must be seriously taken into account when luminescent Eu(III) chelates are used as labels in immunoassays for biomedical applications [55], as biological samples contain ppb of Cu(II) and gross analytical errors may arise from quenching by Cu(II) inducing false positive results. Therefore, the influence of Cu(II) has to be carefully checked for the particular lanthanide label used.

Acknowledgements

S.E.B. and B.C.B. are members of Carrera del Investigador Científico (Research Staff) from CONICET (Consejo Nacional de Investigaciones Científicas y Técnicas, Argentina). We thank Prof. Pedro F. Aramendía for helpful discussions. The work was supported by grants X086 (UBA), PIP 112-200801-02817 and PIP 112-200801-02533 (CONICET, Argentina), and PICT 10621 (ANPCyT, Argentina).

References

[1] C. Yoshina-Ishii, T. Asefa, N. Coombs, J. MacLachlan, A. Ozin, Periodic Mesoporous organosilicas, PMOs: fusion of organic and inorganic chemistry "inside" the channel walls of hexagonal mesoporous silica, Chem. Commun. (1999) 2539–2540.
[2] R.H. Baney, M. Itoh, A. Sakakibara, T. Suzuki, Silsesquioxanes, Chem. Rev. 95 (1995) 1409–1430.
[3] (a) J.S. Beck, J.C. Vartuli, W.J. Roth, M.E. Leonowicz, C.T. Kresge, K.D. Schmitt, C.T.W. Chu, D.H. Olson, E.W. Sheppard, S.B. McCullen, J.B. Higgins, J.L. Schlenker, J. Am. Chem. Soc. 114 (1992) 10834;
(b) B.J. Melde, B.T. Holland, C.F. Blanford, A. Stein, Mesoporous sieves with unified hybrid inorganic/organic frameworks, Chem. Mater. 11 (1999) 3302–3308.
[4] T. Tani, N. Mizoshitaab, Shinji Inagaki, Luminescent periodic mesoporous organosilicas, J. Mater. Chem. 19 (2009) 4451–4456.
[5] E. Benson, A. Medí, C. Reyé, R.J.P. Corriú, Functionalisation of the framework of mesoporous organisilicas by rare-earth complexes, Mater. Chem. 16 (2006) 246–248.
[6] M. Manuela Silva, V. de Zea Bermudez, L.D. Carlos, A. Passos de Almeida, M.J. Smith, Sol–gel processing and structural study of europium-doped hybrid materials, J. Mater. Chem. 9 (1999) 1735–1740.
[7] R. Corriú, A. Mehdi, A.C. Reyé, C. Thieuleux, Control of coordination chemistry in both the framework and the pore channels of mesoporous hybrid materials, New J. Chem. 27 (2003) 905–908.
[8] K. Binnemans, Lanthanide-based luminescent hybrid materials, Chem. Rev. 109 (2009) 4283–4374.
[9] L.D. Carlos, R.A.S. Ferreira, V. de Zea Bermudez, S.J.L. Ribeiro, Lanthanide-containing light-emitting organic–inorganic hybrids: a bet on the future, Adv. Mater. 21 (2009) 509–534.
[10] G.S. Ofelt, Structure of the f^6 configuration with application to rare earth ions, J. Chem. Phys. 38 (1963) 2171–2180.
[11] D. Parker, Excitement in f block: structure, dynamics and function of nine-coordinate chiral lanthanide complexes in aqueous media, Chem. Soc. Rev. 33 (2004) 156–165.
[12] D. Parker, R. Dickins, H. Puschmann, C. Crossland, J. Howard, Being excited by lanthanide coordination complexes: aqua species, chirality, excited-state chemistry, and exchange dynamics, Chem. Rev. 102 (2002) 1977–2010.
[13] R.D Peacock, The intensities of lanthanide f–f transitions, Struct. Bonding 22 (1975) 83–122.
[14] J. Chen, P.R. Selvin, Synthesis of 7-amino-4-trifluoromethyl-2-(1H)-quinolinone and its use as an antenna molecule for the luminescent europium polyaminocarboxylates chelates, J. Photochem. Photobiol. A 135 (2000) 27–32.
[15] P. Ge, P.R. Selvin, Carbostyril, Derivatives as antenna molecules for luminescent lanthanide chelates, Bioconjug. Chem. 15 (2004) 1088–1094.
[16] M. Li, P.R. Selvin, Luminescent polyaminocarboxylate chelates of terbium and europium: the effect of chelate structure, J. Am. Chem. Soc. 117 (1995) 8132–8138.
[17] J-C.G. Bunzli, S. Comby, A.-S. Chauvin, C.D. Vandevyver, New opportunities for lanthanide luminescence, J. Rare Earths 25 (2007) 257–274.
[18] A.-L. Gassner, C. Duhot, J-C.G. Bünzli, A.-S. Chauvin, Remarkable tuning of the photophysical properties of bifunctional lanthanide tris(dipicolinates) and its consequence on the design of bioprobes, Inorg. Chem. 47 (2008) 7802–7812.
[19] T. Liu, J. Hu, J. Yin, Y. Zhang, Ch. Li, Sh. Liu, Enhancing detection sensitivity of responsive microgel-based Cu(II) chemosensors via thermo-induced volume phase transitions, Chem. Mater. 21 (2009) 3439–3446.
[20] G. Winsberg, B.J. Scott, G.D. Stucky, pH Sensing with mesoporous thin films, Chem. Commun. 1 (2001) 119–120.
[21] M. Montalti, L. Prodi, N. Zaccheroni, L. Charbonniere, L. Douce, R. Ziessel, A luminescent anion sensor based on a europium hybrid complex, J. Am. Chem. Soc. 123 (2001) 12694–12695.
[22] S.V. Eliseevaa, J-C.G. Bünzli, Lanthanide luminescence for functional materials and bio-sciences, Chem. Soc. Rev. 39 (2010) 189–227.
[23] C.J. Brinker, G.W. Scherer, Sol–Gel Science, The Physics and Chemistry of Sol–Gel Processing Ac. Press Inc., 1990.
[24] R. Reisfeld, Prospects of sol–gel technology towards luminescent materials, Opt. Mater. 16 (2001) 1–7.
[25] F. Embert, A. Mahdi, C. Reyé, R.J.P. Corriú, Synthesis, Luminescent properties of monophasic organic–inorganic hybrid materials incorporating Europium(III), Chem. Mater. 13 (2001) 4542–4549.
[26] A.-C. Franville, D. Zambon, R. Mahiou, Luminescence behavior of sol–gel derived hybrid materials resulting from covalent grafting of a chromophore unit to different organically modified alkoxysilanes, Chem. Mater. 12 (2000) 428–435.
[27] P. Liu, H. Li, Y. Wang, B. Liu, W. Zhang, Y. Wang, W. Yan, H. Zhang, U. Schubert, Europium complexes immobilization on titania *via* chemical modification of titanium alkoxide, J. Mater. Chem. 18 (2008) 735–737.
[28] R. Hernandez, A.-C. Franville, P. Minoofar, B. Dunn, J.I. Zink, Controlled placement of luminescent molecules and polymers in mesostructured sol–gel thin films, J. Am. Chem. Soc. 123 (2001) 1248–1249.
[29] S. Cousinié, M. Gressier, C. Reber, J. Dexpert-Ghys, M.-L. Menu, Europium(III) complexes containing organosilyldipyridine ligands grafted on silica nanoparticles, Langmuir 24 (2008) 6208–6214.
[30] A. Lobnik, N. Majcen, K. Niederreiter, G. Uray, Optical pH sensor based on the absorption of antenna generated europium luminescence by bromothymolblue in a sol–gel membrane, Sens. Actuators B 74 (2001) 200–206.
[31] N.A.J. Sommerdijk, A. Poppe, C.A. Gibson, J.D. Wright, Unexpected complexation behaviour of a sol–gel immolilised dye: the development of an optical copper(II) sensor, J. Mater. Chem. 8 (1998) 565–567.
[32] J.D. Wright, N.A.C. Higginson, Effects of matrix variation on pH and Cu^{2+} sensing properties of sol–gel entrapped eriochrome cyanine R, J. Mater. Chem. 14 (2004) 201–208.
[33] P.R. Selvin, T.M. Rana, J.E. Hearst, Luminescence resonance energy transfer, J. Am. Chem. Soc. 116 (1994) 6029–6030.
[34] P.R. Selvin, The renaissance of fluorescence resonance energy transfer, Nat. Struct. Biol. 7 (2000) 730–734.
[35] M.A. Kessler, Determination of copper at ng/mL-levels based on quenching of the europium chelate luminescence, Anal. Chim. Acta 364 (1998) 125–129.
[36] P. Brayshaw, J.C.G. Bünzli, P. Froidenaux, J.M. Harrowfield, Y. Kim, A.N. Sobolev, Synthetic, structural, and spectroscopic studies on solids containing tris(dipicolinato) rare earth anions and transition or main group metal cations, Inorg. Chem. 34 (1995) 2068–2076.
[37] L. Zhang, B. Li, Zh. Su, Sh. Yue, Sens. Actuators B Chem. (2010) 595–599.
[38] B. Chen, L. Wang, Y. Xiao, F.R. Fronczek, M. Xue, Y. Cui, G. Qian, Angew. Chem. Int. Ed. 48 (2009) 500–503.
[39] B. Valeur, I. Leray, Design principles of fluorescent molecular sensors for cation recognition, Coord. Chem. Rev. 205 (2000) 3–40.
[40] D. Parker, Luminescent lanthanide sensors for pH, pO_2 and selected anions, Coord. Chem. Rev. 205 (2000) 109–130.
[41] V.B. Bojinov, I. Nikolai, Georgiev, Paula Bosch, Design and synthesis of highly photostable yellow–green emitting 1,8-naphthalimides as fluorescent sensors for metal cations and protons, J. Fluoresc. 19 (2009) 127–139.
[42] O.S. Wolfbeis, Fiber Optic Chemical Sensors and Biosensors, vols. I and II, CRC Press, Boca Raton, 1991.

Please cite this article in press as: B.C. Barja, et al., Luminescent Eu(III) hybrid sensors for in situ copper detection. Sens. Actuators B: Chem. (2011), doi:10.1016/j.snb.2011.06.006

[43] G.M. Murray, R.V. Sarrio, J.R. Peterson, The effects of hydration on the luminescence spectra of the trisodium tris(2,6-pyridenedicarboxylato)europium(III) compounds, Inorg. Chim. Acta 176 (1990) 233–240.
[44] A.-C. Franville, R. Mahiou, D. Zambon, J.-C. Cousseins, Molecular design of luminescent organic–inorganic hybrid materials activated by europium(III) ions, Solid State Sci. 3 (2001) 211–222.
[45] B.C. Barja, P.F. Aramendia, Luminescent Eu(III) hybrid materials for sensor applications, Photochem. Photobiol. Sci. 7 (2008) 1391–1399.
[46] P. Minoofar, B. Dunn, J. Zink, Multiply doped nanostructured silicate sol–gel thin films: spatial segregation of dopants, energy transfer, and distance measurements, J. Am. Chem. Soc. 127 (8) (2005) 2656–2665.
[47] H. Cui, J. Chen, H. Zhou, Y. Lu, Synthesis and infrared and fluorescence spectra of rare earth complexes with a new amide ligand, Spectrochim. Acta A 68 (2007) 478–483.
[48] W.-N. Wu, W.-B. Yuan, N. Tang, R.-D. Yang, L. Yan, Z.-H. Xu, Synthesis, characterizations and luminescent properties of three novel aryl amide type ligands and their lanthanide complexes, Spectrochim. Acta A 65 (2006) 912–991.
[49] N.P.G. Roeges, A Guide to the Complete Interpretation of Infrared Spectra of Organic Structures, John Wiley & Sons Ltd, England, 1994.
[50] R. Reisfeld, E. Zigansky, M. Gaft, Europium probe for estimation of site symmetry in glass films, glasses and crystals, Mol. Phys. 102 (2004) 1319–1330.
[51] B.C Barja, A. Remorino, M.J. Roberti, P.F. Aramendia, Luminescence quenching of europium(III) and terbium carboxylates by transition metals in solution, J. Argentine Chem. Soc. 4/6 (2005) 81–96.
[52] G. Anderegg, Pyridinderivate als Komplexbildner I. Pyridincarbonsauren Helv, Chim. Acta 43 (1960) 414–424.
[53] G. Anderegg, Pyridinderivate als Komplexbildner II. Komplexbildung des dreiwertigen Eisen-Ions mit Pyridincarbonsauren Helv, Chim. Acta 43 (1960) 1530–1545.
[54] I. Grenthe, J. Am. Chem. Soc. 83 (1963) 360.
[55] T. Nishioka, K. Fukui, K. Matsumoto, Lanthanide chelates as luminescent labels in biomedical analysis, in: K.A. Gschneidner Jr., J.-C.G. Bünzli, V.K. Pecharsky (Eds.), Handbook on the Physics and Chemistry of Rare Earths, vol. 37, Elsevier V.B., Amsterdam, 2007, pp. 71–215, Chapter 234.

Biographies

B.C. Barja is a member of the scientific staff of the Instituto de Química Fisica de los Materiales, Medio Ambiente y Energía, Consejo Nacional de Investigaciones Científicas y Técnicas (INQUIMAE/CONICET, Argentina). She obtained her PhD (Physical Chemistry area) at the University of Buenos Aires in 1999. Her research interests focus on the synthesis and development hybrid lanthanide-based luminescent materials with applications in sensing and photoactive materials.

S.E. Bari is a member of the scientific staff of the Instituto de Química Fisica de los Materiales, Medio Ambiente y Energía, Consejo Nacional de Investigaciones Científicas y Técnicas (INQUIMAE/CONICET, Argentina). She holds a PhD degree in Organic Chemistry from the University of Buenos Aires (1991). Her expertise is related to the synthesis, spectroscopic characterization, and study of chemical reactivity of organic molecules and coordination complexes, with bioorganic or bioinorganic relevance.

M.C. Marchi is a professor assistant of the Departamento de Química Inorgánica, Analítica y Química Fisica (DQIAyQF), Facultad de Ciencias Exactas y Naturales (FCEyN)–Universidad de Buenos Aires (UBA). She obtained her PhD (Physical Chemistry area) at the University of Buenos Aires in 2001. Her research interests focus on the synthesis of luminescent semiconductor particles embedded in oxide mesoporous materials to develop solar cells. She possesses large experience in the characterization of nanomaterials by microscopic techniques (TEM SEM).

F. Iglesias is an advanced undergraduate student of the Licenciatura en Ciencias Químicas at the University of Buenos Aires, and has actively collaborated as members in the project X086 (UBA).

M. Bernardi is an advanced undergraduate students of the Licenciatura en Ciencias Químicas at the University of Buenos Aires, and has actively collaborated as members in the project X086 (UBA).

Please cite this article in press as: B.C. Barja, et al., Luminescent Eu(III) hybrid sensors for in situ copper detection. Sens. Actuators B: Chem. (2011), doi:10.1016/j.snb.2011.06.006